Eidgenössische Technische Hochschule Zürich
Swiss Federal Institute of Technology Zurich

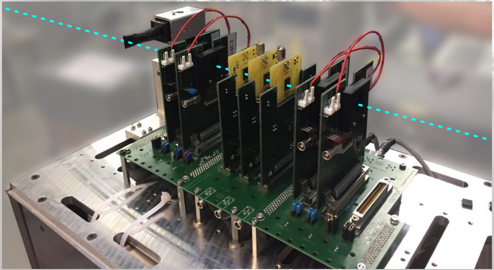

Pulse Height Analysis of 3D pCVD Diamond Detectors

RD42 Meeting

Michael Reichmann

8th May 2019

Table of Contents

Section 1

Introduction

Diamond as Detector Material

- innermost tracking layers $\rightarrow$ highest radiation damage $\mathcal{O}\left(\text{GHz/cm}^2\right)$
- $\rightarrow$ **R&D towards more radiation tolerant detector designs and/or materials**

Diamond as Detector Material

- innermost tracking layers $\rightarrow$ highest radiation damage $\mathcal{O}\left(\mathrm{GHz/cm^2}\right)$
- $\rightarrow$ **R&D towards more radiation tolerant detector designs and/or materials**

Diamond as Detector Material:

- advantageous properties
- **after $1 \cdot 10^{16}\,\mathrm{n/cm^2}$ the mean drift path in diamond larger than in silicon**

Diamond as Detector Material

- innermost tracking layers → highest radiation damage $\mathcal{O}\left(\mathrm{GHz/cm^2}\right)$
- → **R&D towards more radiation tolerant detector designs and/or materials**

Diamond as Detector Material:

- advantageous properties
- **after $1 \cdot 10^{16}\,\mathrm{n/cm^2}$ the mean drift path in diamond larger than in silicon**

Work at ETH:

- investigate signals and radiation tolerance in various detector designs:
  - Pad Detectors → whole diamond as single cell readout
  - Pixel Detectors → diamond sensor on pixel readout chip
  - 3D Pixel Detectors → 3D diamond detector on pixel readout chip

Diamond as Detector Material

- innermost tracking layers → highest radiation damage $\mathcal{O}\left(\mathrm{GHz/cm^2}\right)$
- → **R&D towards more radiation tolerant detector designs and/or materials**

Diamond as Detector Material:

- advantageous properties
- **after $1 \cdot 10^{16}\,\mathrm{n/cm^2}$ the mean drift path in diamond larger than in silicon**

Work at ETH:

- investigate signals and radiation tolerance in various detector designs:
  - Pad Detectors
  - Pixel Detectors
  - **3D Pixel Detectors** → this talk

Detectors

	II6-A2	II6-B6
manufacturer	II-VI Inc.	II-VI Inc.
diamond type	poly-crystal	poly-crystal
size	∼4 mm × 4 mm	∼4 mm × 4 mm
thickness	∼500 μm	455 μm
irradiation	none	none
construction	summer 2016	summer 2017
3D drilling	Oxford	Oxford
3D cell size	150 μm × 100 μm	50 μm × 50 μm
columns	20 × 30 **(600)**	60 × 62 **(3720)**
pixel chip	PSI46digV2.1respin (CMS)	PSI46digV2.1respin (CMS)
pixel pitch	150 μm × 100 μm	150 μm × 100 μm
ganged cells	1 × 1	2 × 3 (6 cells)
bump & wire bonding	Princeton	Princeton

Table: 3D Pixel Detector Properties.

Detectors

	II6-A2	**II6-B6**
manufacturer	II-VI Inc.	II-VI Inc.
diamond type	poly-crystal	poly-crystal
size	$\sim$4 mm $\times$ 4 mm	$\sim$4 mm $\times$ 4 mm
thickness	$\sim$500 μm	455 μm
irradiation	none	none
construction	summer 2016	summer 2017
3D drilling	Oxford	Oxford
3D cell size	150 μm $\times$ 100 μm	50 μm $\times$ 50 μm
columns	20 $\times$ 30 **(600)**	60 $\times$ 62 **(3720)**
pixel chip	PSI46digV2.1respin (CMS)	PSI46digV2.1respin (CMS)
pixel pitch	150 μm $\times$ 100 μm	150 μm $\times$ 100 μm
ganged cells	1 $\times$ 1	2 $\times$ 3 (6 cells)
bump & wire bonding	Princeton	Princeton

Table: 3D Pixel Detector Properties.

- II6-A2 broke in October 2016 (chip malfunctioned) $\rightarrow$ successful re-bonding
- II6-B6 has long history of breaking ...

Measurements

	Oct 16	May 17	Aug 17	Sep 18	Oct 18	Nov 18
place	PSI	PSI	PSI	CERN	CERN	PSI
II6-A2	✓	✓	✓	✓	✓	✓
II6-B6	✗	✗	✓	✓	✓	✓

Table: 3D Pixel Detector Measurements.

- standard rate and voltage scans
- rise time scans: change of amplifier rise time at fixed flux and voltage
- angle scans: change of incident angle at fixed flux and voltage

Measurements

	Oct 16	**May 17**	**Aug 17**	**Sep 18**	**Oct 18**	**Nov 18**
place	PSI	PSI	PSI	CERN	CERN	PSI
II6-A2	✓	✓	✓	✓	✓	✓
II6-B6	✗	✗	✓	✓	✓	✓

Table: 3D Pixel Detector Measurements.

- standard rate and voltage scans
- rise time scans: change of amplifier rise time at fixed flux and voltage
- angle scans: change of incident angle at fixed flux and voltage

History of II6-B2:

- 06/2017 - sensor processing and detector fabrication
- 08/2017 - first measurement $\rightarrow$ wrong chip calibration $\rightarrow$ high threshold ($\sim$10 ke)
- 04/2018 - several pixels malfunction $\rightarrow$ re-bump-bonding to new chip
- 06/2018 - sensor detaches while shipping $\rightarrow$ re-bump-bonding, fixate with silguard
- 11/2018 - efficiency worsens and sensor detaches again

Section 2

3D Pixel Detector

Diamond as Particle Detector

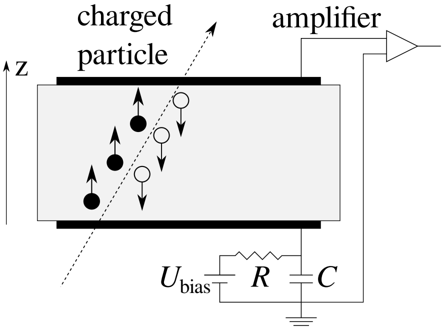

(a) Detector Schematics

(b) 15 cm ⌀ pCVD Diamond Wafer

- detectors operated as ionisation chambers
- metallisation on both sides
- poly-crystals produced in large wafers

Working Principle

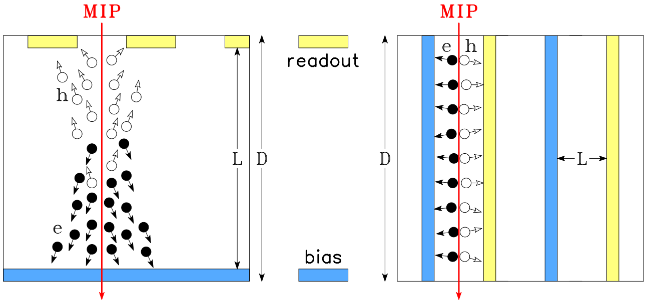

- after large radiation fluence all detectors become trap limited
- bias and readout electrode inside detector material
- same thickness D → same amount of induced charge → shorter drift distance L
- **increase collected charge in detectors with limited mean drift path (Schubweg)**

Bump Bonding

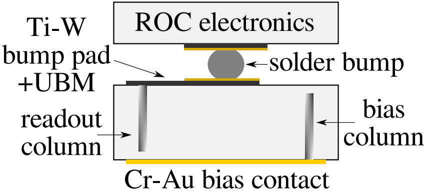

(a) Bump bond schematics

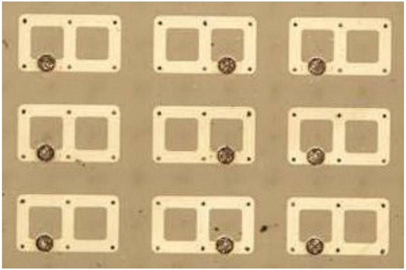

(b) 3×2 bump pads

- electrodes (columns) drilled with femto-second laser
- connection to bias and readout with surface metallisation
- ganging of cells to match pixel pitch of readout-chip (ROC)
- small gap ($\sim$15 μm) to the surface to avoid a high voltage break-through

Section 3

Pulse Height Calibration

Pixel Unit Cell

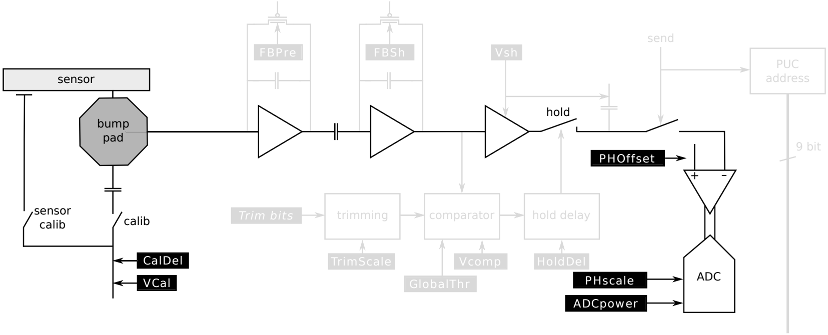

- inject calibration signal ($\sim$vcal) through sensor into same circuit as real signals
- shaping, amplification, threshold check
- set amplification offset
- convert to 8 bit adc value with adjustable scale $\rightarrow$ readout

ADC Calibration

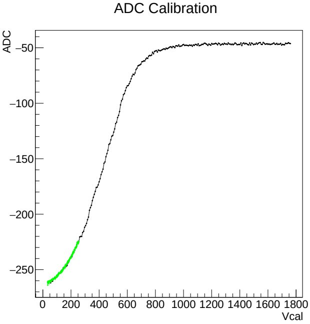

(a) ADC calibration for single pixel.

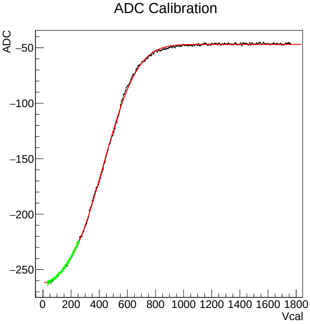

(b) Error function fit.

- measure adc values for calibration pulses with different vcal
- adc follows error function and saturates for high vcal
- fit every pixel and save fit parameters
- adjust adc offset and range with DACs of the chip

Vcal Calibration

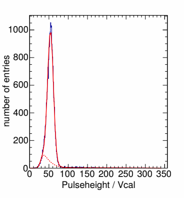

(a) Zn target.

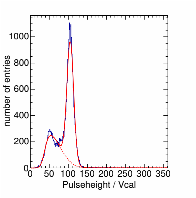

(b) Mo target.

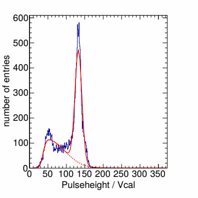

(a) Ag target.

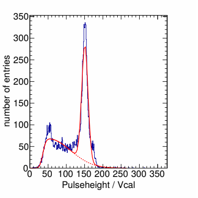

(b) Sn target.

- measure energy spectra of K_α lines of four metal targets using ADC-calibration

Vcal Calibration

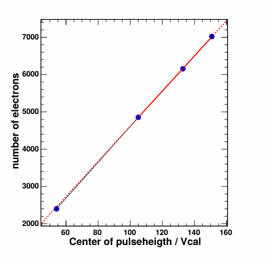

Figure: Vcal Calibration.

- measure energy spectra of K_α lines of four metal targets using ADC-calibration
- linear dependence of energy [e] and vcal
- fit K_α points with straight line (similar for each chip)
- impossible to do calibration with diamond (energy too low)

Vcal Calibration

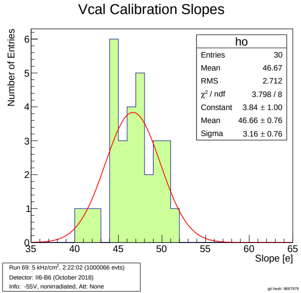

(a) Vcal slopes.

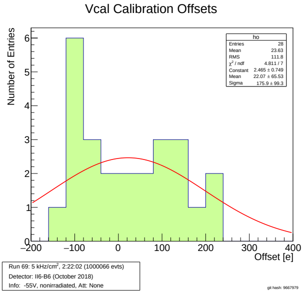

(b) Vcal offsets.

- measure energy spectra of K_α lines of four metal targets using ADC-calibration
- linear dependence of energy [e] and vcal
- fit K_α points with straight line (similar for each chip)
- impossible to do calibration with diamond (energy too low)
  - use general values from silicon: $\mathrm{e} = 46.5 \cdot vcal$

Section 4

Analysis

Cuts

Cut	Excluded Events
event range	first minute of the run due to various beam conditions
beam interruptions	during rate changes of the beam due to beam interruption
aligned	DUT and Telescope are not aligned (event-wise)
trigger phase	Chip trigger timing is incorrect
tracks	not all telescope planes have exactly one cluster
chi2 (x/y)	badly fit tracks (>50 % quantile)
track slope (x/y)	large angles of the tracks (>2 deg)
rhit	large DUT residual (>100 mm)
pixel mask	noisy pixels
fiducial	not in selected (fiducial) area of the DUT

Table: Analysis cut flow.

- cuts applied in order of the table
- largest contribution usually by chi2, tracks and fiducial cuts

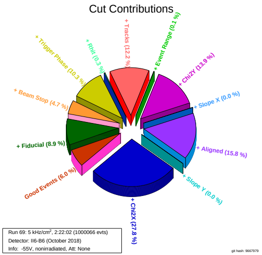

Section 5

Conclusion

Conclusion

- empty
- moreempty
- moremoreempty

Del Fin